Int J Adv Manuf Technol (2015) 79:197–210
DOI 10.1007/s00170-015-6823-x

ORIGINAL ARTICLE

Tool damage and machined-surface quality using hot-pressed sintering $Ti(C_7N_3)$/WC/TaC cermet cutting inserts for high-speed turning stainless steels

Bin Zou · Huijun Zhou · Chuanzhen Huang · Kaitao Xu · Jun Wang

Received: 16 September 2014 / Accepted: 18 January 2015 / Published online: 1 February 2015

Abstract A $Ti(C_7N_3)$/WC/TaC cermet cutting tool was developed using a hot-pressed technology. A standard orthogonal array was used to investigate the cutting performance of this newly developed insert in the high-speed turning of 17-4PH martensitic and 321 austenitic stainless steels. The effects of the cutting parameters on the tool life and surface quality were analysed to examine the performance of the inserts based on Taguchi method. The mechanisms of tool damage and machined-surface generation and their relationships were also thoroughly discussed to understand the machinability of different stainless steels. The used cutting parameters are as follows: a cutting speed of 350~400 m/min for 17-4PH steel and 300~350 m/min for 321 steel and a feed of 0.10 mm/r and a depth of cut of 0.30~0.35 mm, which is considered to be a notably efficient parameter for machining stainless steel. The crater wear and flank wear prevailed in the machining of 17-4PH martensitic stainless steel, whereas the flank wear was serious and edge chipping occurred in the machining of 321 austenitic stainless steel. There were some pits on the machined-surfaces of 17-4PH steel and some material side flow on the machined-surface of 321 steel, which is related with the e material properties of these two stainless steels.

B. Zou · H. Zhou · C. Huang · K. Xu · J. Wang
Centre for Advanced Jet Engineering Technologies (CaJET), School of Mechanical Engineering, Shandong University, Jinan 250061, People's Republic of China

B. Zou · H. Zhou · C. Huang · K. Xu · J. Wang
Key Laboratory of High Efficiency and Clean Mechanical Manufacture, Ministry of Education, Shandong University, Jinan, People's Republic of China

B. Zou (✉)
Shandong University, 17923 Jing Shi Road, Jinan 250061, People's Republic of China
e-mail: zou20011110@163.com

Keywords $Ti(C_7N_3)$ · Cutting inserts · Tool damage · Machined-surface · Stainless steel

1 Introduction

Stainless steel belongs to a difficult-to-cut material in high-speed machining. The cutting inserts recommended by tool manufacturers are usually coated cemented carbide inserts. The ultrafine/nano Ti(C,N)-based cermet was likely to enlarge the field of cutting-tool materials because this cutting tool exhibited better wear, better oxidation resistance, and even a longer service life [1]. Ti(C,N) cermet cutting tools are more suitable to machine normal steel and iron materials than ceramic cutting tools because of their lower hardness [2, 3]. The defects of hardness and abrasion of Ti(C,N)-based cermets can be offset by adding some hard carbides, such as WC and TaC. The machining time was reduced from 7 to 2.5 h, and its cost was reduced by 75 % when a Ti(C,N) cermet cutting insert was used to machine 86CrMoV hardened-steel rollers with a hardness of HRC58-63 [4]. Ti(C,N) cermet cutting tools with the addition of 20 wt% WC had the longest tool life in machining of AISI 45 steel [5]. 17-4PH stainless steel belongs to a hard-to-cut material because of its low thermal conduction and high ductility [6]. 321 austenitic stainless steel is also considered as a difficult-to-cut material because of its high friction coefficient, low thermal conductivity, high coefficient of thermal expansion, high ductility and high work hardening rate [7]. The range of traditional cutting speeds is 200–350 m/min when stainless steel is machined using coated cemented carbides inserts. The machined-surface of austenitic stainless steel cut at the cutting speed of above 450 m/min showed an evidence of material side flow [8], and the values of machined-surface were similar at high and low cutting speeds, which yielded a minimum Ra value of 1.66 μm at 600 m/min.

In this study [8], the duration that the cutting inserts could maintain at these high cutting speeds was not provided, although some tool wear mechanisms were investigated. A commercially available TiAlN-coated carbide tool was used to perform a hard turning of martensitic stainless steel with a hardness of 47–48 HRC [9]. They set the criteria of tool life at a maximum width of flank wear as 0.14 mm or sever tool breakage and reported that the longest tool life was approximately 31 min when the cutting speed was 130 m/min, the feed was 0.1 mm/r and the depth of cut was 0.4 mm; however, the shortest tool life was 3 min at a cutting speed of 170 m/min, feed of 0.16 mm/r and depth of cut of 0.4 mm. Gerth et al. [10] investigated the adhesion between the chip and the tool rake face using hard ceramic-coated cemented carbide inserts to turn the austenitic stainless steel (316L) and carbon steel (UHB11) at a cutting speed of 150 m/min and feed of 0.154 mm/r, and demonstrated that the stainless steel was more adhered than the carbon steel. This study did not investigate the adhesion phenomena that resulted from the higher cutting speeds. A feed range of 0.2~0.28 mm/r had a greater effect on the surface roughness, and a cutting speed range of 30~100 m/min had a greater effect on the tool wear when AISI 304 austenitic stainless steel was machined using carbide cemented inserts in cutting fluids [7]. The Ra surface roughness of 0.37 μm was obtained when X6CrNiTi18-10 austenitic stainless steel was machined at a cutting speed of 140 m/min, feed of 0.17 mm/r and depth of cut of 0.27 mm [11]; this result even satisfied the grinding operation demands in high-quality part production.

Most used cutting tools for machining stainless steel were cemented carbide inserts, and the cutting efficiency was not high because the selected cutting parameters were low. Some researchers investigated the cutting phenomena, such as the cutting heat, cutting forces and chips, at a notably high cutting speed (above 300~400 m/min), but manufactures would rather not apply these parameters because of the short cutting times. There are relatively few studies on cermet tools of machined stainless steel because there is no confidence in the performance of cermet tools. In our work, a new Ti(C_7N_3)/WC/TaC cermet tool material was developed using a hot-pressed sintering technology and subsequently manufactured into inserts by grinding. The cutting performances of this insert were investigated in high-speed turning of two types of stainless steel (17-4PH marstentic and 321 austentic) at different cutting parameters, which were planned using the Taguchi method. The cutting efficiencies, tool life and surface toughness were analysed to examine the values of this newly developed cutting tool for engineering applications and scientific values. The mechanisms of tool damage, machined-surface generation and their relationships were also thoroughly discussed to lay some foundations for improving the machining efficiencies and enlarge the machinability of stainless steels.

2 Material design and experimental methods

Ti(C_7N_3)/WC/TaC cermet cutting inserts were manufactured by three steps. First, the compact cermet disks were sintered using a hot-pressing technology in a graphite die in vacuum at 1400 °C under a pressure of 30 MPa with a holding time of 30 min. Second, these hot-pressed disks were cut into rectangular tool blanks of 7 mm×22 mm×22 mm by electrospark wire-electrode cutting. Third, the tool blanks were ground and polished into cutting inserts of 6 mm×20 mm×20 mm to improve their surface smoothness and reduce the friction between the tools and the workpiece materials. The tool edges were also chamfered to avoid tipping, and their chamfer angle and width were −15° and 0.1 mm, respectively. The tool noses were rounded into a radius of 0.3 mm to enhance the impact resistance and avoid a sudden collapse at the beginning of machining. The other effective geometries of the inserts after rigid clamping in the tool post are as follows: rake angle of −5°, relief angle of 5°, inclination angle of −5° and edge angle of 45°. The mechanical properties of our hot-pressed sintered inserts are listed in Table 1. The cutting experiments were performed under cooling conditions on a PUMA200MA turning centre. Two types of stainless steels (17-4PH martensitic stainless steel and 321 austenitic stainless steel) were selected as the workpiece materials to evaluate the cutting performance of our developed cermet inserts. The chemical compositions and mechanical properties of these two stainless steels are listed in Tables 2 and 3. These two stainless steels contain a high Cr content and have good mechanical properties, which determine that they belong to the category of difficult-to-cut materials.

An L9(3^4) orthogonal test with three factors (cutting speed, feed and depth of cut) was designed in Table 4 to evaluate the cutting performance of these cutting inserts. The independent parameter variables were the cutting speed, feed and depth of cut, each of which had three levels: the cutting speed was 300, 350 and 400 m/min; the feed was 0.10, 0.15 and 0.20 mm/r and the depth of cut was 0.25, 0.30 and 0.35 mm. According to the Taguchi design method, a standard L9(3^4) orthogonal array was applied in Table 5, where the cutting speed, feed and depth of cut were set as factors A, B and C, respectively, and factor D was set as the empty column. The tool wear widths were measured using a handheld microscope

Table 1 Mechanical properties of our hot-pressed sintering Ti(C_7N_3)/WC/TaC cermets cutting inserts

Flexural strength (MPa)	Fracture toughness (MPa·$m^{1/2}$)	Hardness (HV20, GP)	Relative density (%)
1759	6.07	18.55	99.4

Table 2 Chemical compositions and mechanical properties of 17-4PH martensitic stainless steel

17-4PH martensitic stainless steel	
Composition (wt%)	
Fe	Bal
Cr	15.80
Ni	3.78
Cu	3.12
Mn	0.68
Si	0.47
C	0.044
P	0.038
S	0.004
Ta+Nb	0.17
Mechanical properties	
Yield strength (MPa)	1235
Tensile strength (MPa)	1435
Elongation (%)	12
Reduction of area (%)	45
Hardness (HRC)	43

(AMT413ZT, Diguang, Taiwan). After each test, the worn cutting inserts were measured using an optical microscope to determine the degree of flank wear at an interval of 5 min. The width of the flank-wear criterion was taken as 0.3 mm or catastrophic failure. The topographies and microstructure of tool wear and finished surface were observed using a laser scanning microscope (LSM, VK-X200K, Keyence, Japan), scanning electron microscopy and energy-dispersive spectroscopy (SEM and EDS, SUPRA55, Germany).

Table 3 Chemical compositions and mechanical properties of 321 austenitic stainless steel

321 austenitic stainless steel	
Composition (wt %)	
Fe	Bal
Cr	17.24
Ni	8.10
Mn	0.94
Si	0.60
Ti	0.29
C	0.045
P	0.033
S	0.001
Mechanical properties	
Yield strength (MPa)	217
Tensile strength (MPa)	534
Elongation (%)	44
Reduction of area (%)	53
Hardness (HBS)	189

Table 4 Experimental parameters and levels

Symbols	Cutting parameters	Level 1	Level 2	Level 3
A	Cutting speed (m/min)	300	350	400
B	Feed (mm/r)	0.10	0.15	0.20
C	Depth of cut (mm)	0.25	0.30	0.35

3 Results and discussion

3.1 Analysis of orthogonal test

The range analysis of tool life and finished surface roughness in turning of two stainless steels is provided in Tables 6 and 7. The longest tool life was obtained with the lowest cutting parameters of A1 (300 m/min), B1 (0.10 mm/r) and C1 (0.25 mm) to turn 17-4PH martensitic stainless steel, whereas there was a slight difference in turning 321 austenitic stainless steel because of the longer life at the cutting speed of A1 (300 m/min), feed of B1 (0.10 mm/r) and depth of cut of C2 (0.30 mm). For turning the 17-4PH martensitic stainless steel, the cutting parameters of A3 (400 m/min), B1 (0.10 mm/r) and C1 (0.25 mm) smoothened the finished surface, whereas the cutting parameters of A1 (300 m/min), B1 (0.10 mm/r) and C2 (0.30 mm) reached the smoother surface when the 321 austenitic stainless steel was turned.

A relationship of targets (tool life) with the cutting speed, feed and depth of cut is given in Fig. 1 based on Tables 6 and 7 according to the Taguchi Method [12]. Though variation trends of targets (tool life) with factors (three cutting parameters) are displayed in Fig. 1, it is difficult to distinguish the degree of influences of the different factors on the targets because the variation range of the feed is larger than the other two parameters. To overcome these disadvantages, a mathematical formula was deduced. According to the metal cutting principle [3],

Table 5 Experimental layout using an L9(3^4) orthogonal array

Experimental numbers	Cutting parameter levels			
	A	B	C	D
No. 1	1	1	1	1
No. 2	1	2	2	2
No. 3	1	3	3	3
No. 4	2	1	2	3
No. 5	2	2	3	1
No. 6	2	3	1	2
No. 7	3	1	3	2
No. 8	3	2	1	3
No. 9	3	3	2	1

Table 6 Analysis of range of the results after turning 17-4PH martensitic stainless steel

Numbers		Cutting speed (m/min)	Feed (mm/r)	Depth of cut (mm)	Empty column	Tool life (min)	Finished surface roughness (um)
No. 1		1 (300)	1 (0.10)	1 (0.25)	1	169	0.58
No. 2		1	2 (0.15)	2 (0.30)	2	62	1.44
No. 3		1	3 (0.20)	3 (0.35)	3	14	2.14
No. 4		2 (350)	1	2	3	81	0.80
No. 5		2	2	3	1	18	1.42
No. 6		2	3	1	2	17	2.24
No. 7		3 (400)	1	3	2	46	0.70
No. 8		3	2	1	3	24	1.00
No. 9		3	3	2	1	9	2.31
Tool life (min)	K_1	245	296	210	196	∑= 440	
	K_2	116	104	152	125		
	K_3	79	40	78	119		
	k_1	82	99	70			
	k_2	39	35	50			
	k_3	26	13	26			
	Range	56	86	44			
	Sequence	A_1	B_1	C_1			
Finished surface roughness (um)	K_1	4.16	2.08	3.82	4.31	∑=12.63	
	K_2	4.46	3.86	4.55	4.38		
	K_3	4.01	6.69	4.26	3.94		
	k_1	1.39	0.69	1.27			
	k_2	1.49	1.29	1.52			
	k_3	1.34	2.23	1.42			
	Range	0.15	1.54	0.25			
	Sequence	A_3	B_1	C_1			

the experimental for tool life as function of cutting parameters is:

$$T = Cv^a f^b a_p^c \tag{1}$$

where T is the tool life, c is constant, and v, f and a_p is the cutting speed, feed and depth of cut, respectively. Based on datum in Tables 6 and 7, two mathematical expressions can be regressed by programming and fitting using the Matlab software as the following:

$$T = e^{14.45} v^{-3.14} f^{-2.72} a_p^{-1.74} \quad \text{for 17-4PH martensitic stainless steel} \tag{2}$$

$$T = e^{18.66} v^{-3.14} f^{-1.70} a_p^{0.58} \quad \text{for 321 austenitic stainless steel} \tag{3}$$

It is seen from Eqs. (2) and (3) that an increase of the cutting speed reduced the tool life to the maximum extent due to its exponents more than the others. The larger gap between the exponents of the cutting speed and the feed for machining 321 austenitic than 17-4PH martensitic stainless steels illuminates that the cutting speed predominated the tool life among three cutting parameters in machining of 321 austenitic stainless steel. An increase of the depth of cut depressed the tool life in machining of 17-4PH martensitic stainless steel but availed the tool life to some extent in machining of 321 austenitic stainless steel. The workpiece bar was cut continuously during our experiment and the machined-surface in this cut acted as the unfinished surface in the next cut. It is general for work-hardening of the machined-surface in machining of some materials containing Ni and Cr elements. The improvement of the depth of cut to a certain extent employed the cutting edge kept away from the work-hardening layer in machining of 321 austenitic stainless steel, and thus, the cutting edge was protected from an impact with the hardened layer. However, it is concluded that the work-hardening was heavier on the machined-surface of 321 austenitic than 17-4PH martensitic stainless steels during machining.

A relationship of targets (surface roughness) with the cutting speed, feed and depth of cut is given in Fig. 2 based on Tables 6 and 7 according to the Taguchi Method [12]. It is seen from that the value of surface roughness increased with

Table 7 Analysis of range of the results after turning 321 austenitic stainless steel

Numbers		Cutting speed (m/min)	Feed (mm/r)	Depth of cut (mm)	Empty column	Tool life (min)	Finished surface roughness (um)
1		1 (300)	1 (0.10)	1 (0.25)	1	64	0.60
2		1	2 (0.15)	2 (0.30)	2	34	1.25
3		1	3 (0.20)	3 (0.35)	3	28	2.45
4		2 (350)	1	2	3	57	0.75
5		2	2	3	1	31	2.37
6		2	3	1	2	18	3.15
7		3 (400)	1	3	2	34	0.95
8		3	2	1	3	14	1.50
9		3	3	2	1	9	2.56
Tool life (mm)	K_1	126	155	96	104	∑=289	
	K_2	106	79	100	86		
	K_3	57	55	93	99		
	k_1	42	52	32	–		
	k_2	35	26	33	–		
	k_3	19	18	31	–		
	Range	23	34	2	–		
	Sequence	A_1	B_1	C_2	–		
Finished surface roughness (um)	K_1	4.30	2.30	5.25	5.53	∑=15.58	
	K_2	6.27	5.12	4.56	5.35		
	K_3	5.01	8.16	5.77	4.7		
	k_1	1.43	0.77	1.75	–		
	k_2	2.09	1.71	1.52	–		
	k_3	1.67	2.72	1.92	–		
	Range	0.66	1.95	0.40	–		
	Sequence	A_1	B_1	C_2	–		

the feed despite of the variation range of the feed is larger than that of the other two parameters. The effects of the cutting speed, feed and depth of cut on the surface roughness and material removal rate during turning of X20Cr13 stainless steel were investigated using a Taguchi experimental design method demonstrated by Lakhdar et al. [13], and found that the cutting speed and depth of cut had less influences on the surface roughness, whereas a rise in feed increased the surface roughness by using grey relational analysis. The improvement of feed causes a poor surface roughness and has the most dominant effect on the surface roughness, which obeys the traditional law of turning operation [13]. On the other hand,

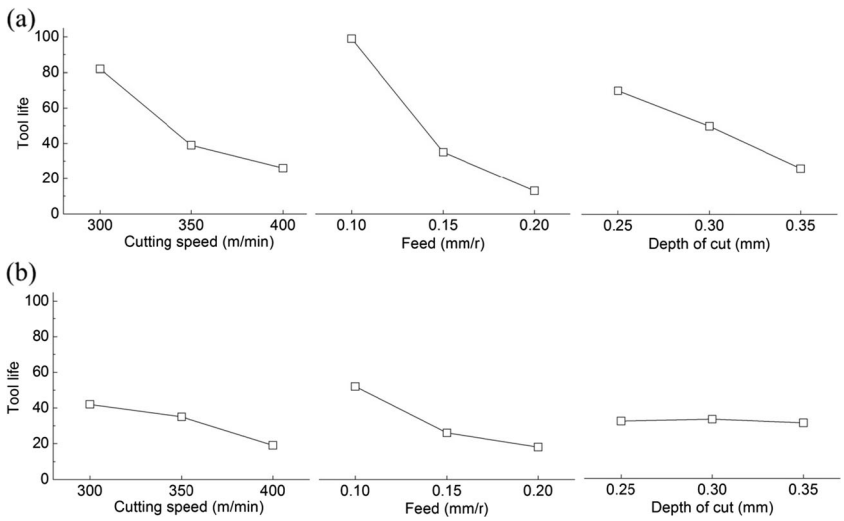

Fig. 1 Relationship of target (tool life) with factors (three cutting parameters) in machining of **a** 17-4PH martensitic and **b** 321austenitic stainless steels according to Tables 6 and 7

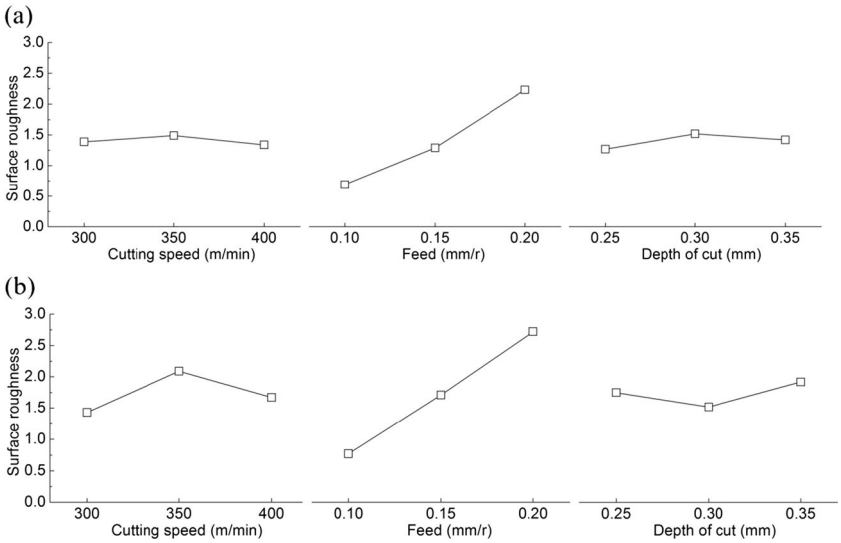

Fig. 2 Relationship of target (machined-surface roughness) with factors (three cutting parameters) in machining of **a** 17-4PH and **b** 321 stainless steels according to Tables 6 and 7

the cutting speed and the depth of cut have the small impacts on the surface roughness in machining of 17-4PH martensitic stainless steel. Farshid et al. [14] also reported that the lower value of the surface roughness was obtained in the highest cutting speed and moderate range of depth of cut by using an ANN model. However, the increasing cutting speed could make the surface roughness worse in machining of 321 austenitic stainless steel, and it implies that topographies of the machined-surface may be changed.

Considering this analysis comprehensively, a cutting speed of 350~400 m/min, a feed of 0.10 mm/r and a depth of cut of 0.30~0.35 mm were selected to machine 17-4PH martensitic stainless steel, the machined-surface roughness of which was less than 1.0 μm, and the tool life was more than 46 min. For 321 austenitic stainless steel, a cutting speed of 300~350 m/min, a feed of 0.10 mm/r and a depth of cut of 0.30~0.35 mm provided a surface roughness of less than 1.0 μm and a tool life of more than 34 min. However, for all of the cutting parameters in this orthogonal test, the longest tool life and the best surface roughness were 169 min and 0.58 μm, respectively, when the 17-4PH martensitic stainless steel was machined, and were 64 min and 0.60 μm, respectively, when the 321 austenitic stainless steel was machined. In this case, the cutting parameters were as follows: a cutting speed of 300 mm/min, a feed of 0.1 mm/min and a depth of cut of 0.25 mm.

3.2 Tool damage

The above discussion have classified that the larger depth of cut and lower cutting speed are beneficial to tool life, and the faster feed worsen the machined-surface roughness in machining of 321 austenitic stainless steel. Therefore, one more group of cutting parameters (v=300 m/min, f=0.10 mm/r, a_p=0.35 mm) was established for machining of the 321 austenitic stainless steel. Figure 3 shows the changes of the tool wear rate with the cutting time in machining two stainless steels at four groups of cutting parameters, which were selected based on the above analysis. When the 17-4PH martensitic stainless steel was machined at a cutting speed of 400 m/min, a feed of 0.10 mm/r and a depth of cut of 0.35 mm, the tool flank suddenly collapsed after a stable wear of 46 min, whereas the flank wear slowly increased to 0.3 mm for 85 min at a cutting speed of 350 m/min, a feed of 0.10 mm/r and a depth of cut of 0.30 mm. A longer turning time, which is more than 2.5 h, could be obtained when this steel was machined at a cutting speed of 300 m/min, a feed of 0.10 mm/r and a depth of cut of 0.25 mm (see Table 6), which indicates that our developed cutting inserts have excellent cutting performance to turn this stainless steel. For the 321 austenitic stainless steel, the tool flank suffered from a stable wear in the first 40 min and subsequently entered a stage of fast wear until the sixtieth minute. Similar wear variations appeared, and our developed inserts exhibited good cutting performance with these parameters when machining the 321 austenitic stainless steel (v=300 m/min, f=0.10 mm/r and a_p=0.35 mm and v=350 m/min, f=0.10 mm/r, a_p=0.30 mm). However, the flank wear exceeded 0.3 mm within 5 to 7 min after its width became 0.22 mm. Furthermore, the tool life was prolonged for only 10~12 min if the cutting parameters were reduced to a cutting speed of 300 m/min, a feed of 0.10 mm and a depth of 0.25 mm, which was far less than the tool life of 169 min when machining the 17-4PH martensitic stainless steel (see Tables 6 and 7). For another set of cutting parameters (v=350 m/min, f=0.10 mm/r, a_p=0.30 mm), the tool life when machining the 321 austenitic stainless steel was three fourths of that when machining the 17-4PH martensitic stainless steel. The tool life when machining the 17-4PH steel increases because of the lower cutting parameters, but this phenomenon was not obvious when the 321 steel was machined, which was discussed in the following sections.

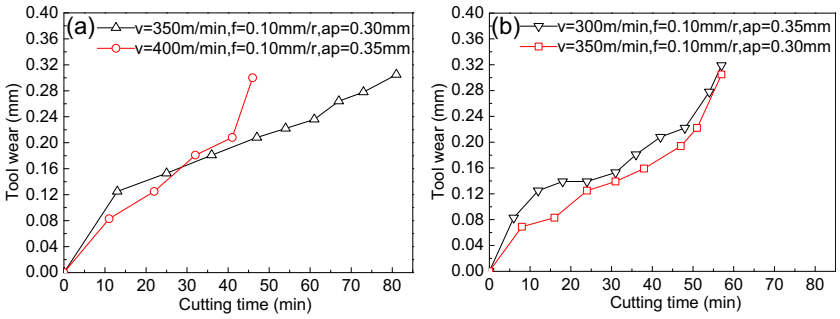

Fig. 3 Tool wear vs. the cutting time in machining of 17-4PH martensitic and 321 austenitic stainless steels at a cutting speed of 300~400 mm/min, feed of 0.1 mm/min and depth of cut of 0.30~0.35 mm

Though the criterion of tool life was determined by the flank-wear width in this work, the tool damage was observed from its rake face and flank face, and its detailed mechanisms were analysed in order to understand the reason of high performance of our developed inserts. Figure 4 shows the LSM topographies of the rake face of worn inserts when machining 17-4PH martensitic stainless steel at different cutting parameters that correspond to Fig. 3a. Both two- and three-dimensional micrographs are provided. Some craters and notches were engendered on the rake faces, and their depths were measured in two mutually perpendicular directions. The depths and shapes of the craters varied with the cutting parameters. The crater was located in front, near the tool noses on the rake face in Fig. 4a (v=350 m/min, f=0.10 mm/r, a_p=0.30 mm), and its maximum depth was approximately 50~60 μm. The notch, which was located on the cutting edge, was originally apart from the crater on the rake face. However, in Fig. 4b, the notch connected to the crater (v=400 m/min, f=0.10 mm/r, a_p=0.35 mm). In this case, the crater approached the cutting edge, and its depth reached 150 μm on the cutting edge. Shaw [3] demonstrated that the tool temperature and the crater depth abruptly increased when the crater approached the cutting edge. In this work, the tool face around the crater was burned to black, which implies that the insert endured a notably heavy heat load during machining. The cutting speed and depth of cut increased by 14 % (from 350 to 400 m/min and from 0.30 to 0.35 mm, respectively); the tool damage was so heavy that the tool life was reduced approximately by 44 %. To further analyse the mechanism of tool damage in machining the 17-4PH martensitic stainless steel, SEM micrographs and EDS spectrums of the worn flank face are shown in Fig. 5 (v=400 m/min, f=0.10 mm/r, a_p=0.35 mm). Although the

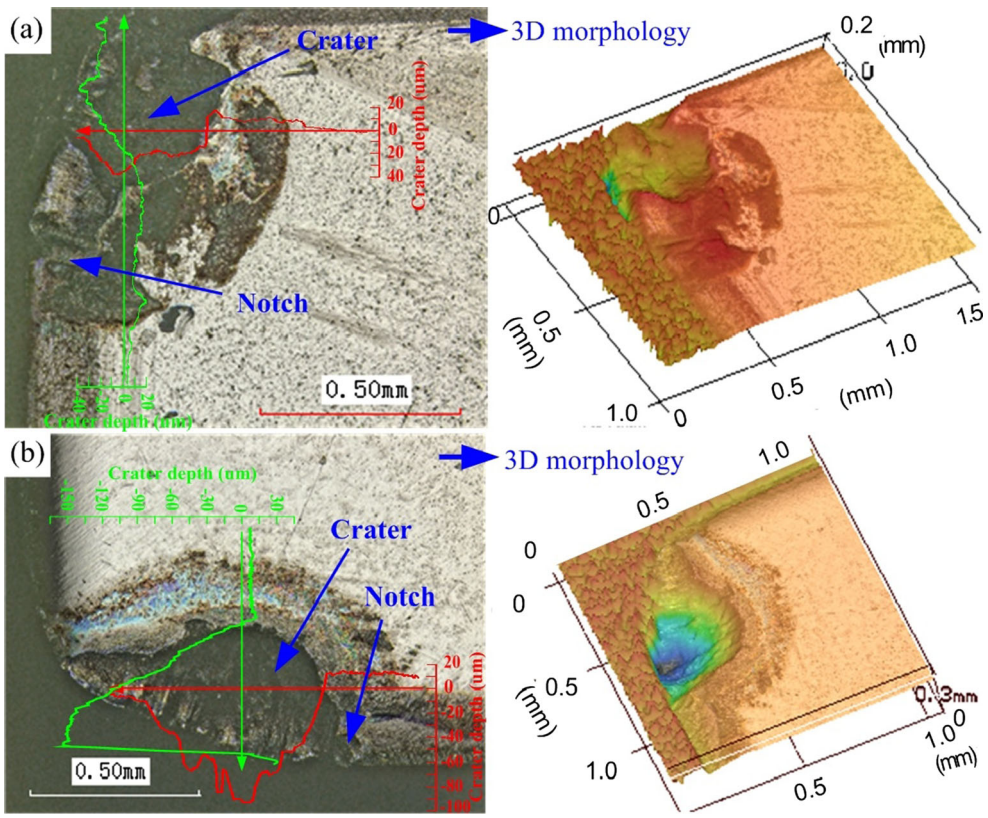

Fig. 4 LSM topographies of the damage on the rake face of the inserts when machining 17-4PH martensitic stainless steel at **a** v=350 m/min, f=0.10 mm/r and a_p=0.30 mm and **b** v=400 m/min, f=0.10 mm/r and a_p=0.35 mm

conditions on the rake face are generally much severer than those on the flank face, the flank face was also seriously damaged. In the view of the flank face, the crater on the rake face is observed, which indicates that the cutting edge was worn out. A region below the cutting edge was magnified in Fig. 5b, and its EDS patterns identified that some Fe, Ni, Mn and Cr elements were adhered on the worn flank face. When a stronger bond than the local strength of the cutting edge was established between the adhesive workpiece material and the tool material, the tool material was torn and the edge was subsequently worn away, which is a main reason of tool failure in machining the 17-4PH martensitic steel. The SEM and EDS patterns of another selected region reveal a characteristic abrasive wear on the worn flank face (see Fig. 5c, e). No obvious grooves and ridges were observed in this region, but two cracks were generated perpendicular to the scratch direction. The crack formation was ascribed to the high cutting temperature, which was produced by the rubbing of the cutting edge, and a friction force, which originated from the flank face in contact with the machined-surface during machining. Because the crack remained away from the serious adhesive region, the tool was bound to suddenly fracture if the adhesive wear diffused to the crack regions. Fortunately, the tool breakage did not result from these abrasive and adhesive wear before the criterion of the flank-wear width was attained.

Figure 6 shows the LSM topographies of the rake face of the worn inserts when machining 321 austenitic stainless steel using different cutting parameters that correspond to Fig. 3b. The 3D morphology reveals that the damage rake surface did not display a heavy crater but a cutting edge chipping, which distinguished from the damage rake face in machining 17-4PH martensitic stainless steel. The tool life may be reduced immediately before total destruction because of this edge chipping. A heavy notch was maintained on the cutting edge, as shown in the 3D morphology of Fig. 6b at a cutting speed of 350 m/min, a feed of 0.10 mm/r and a depth of cut of 0.30 mm, and its maximum depth reached 150 um. The SEM micrographs and EDS spectrums of the flank damages are shown in Figs. 7 and 8, respectively. In the view of the flank face, obvious edge chipping was observed. A chipping region was magnified to find that some Ti(C,N) grains were exited from their roots in Fig. 7b, d, which was a characteristic facture pattern of tool materials [15, 16]. Some heavy grooves and ridges were observed on the flank face (see Fig. 7a), and some elements of the workpiece materials diffused into the flank face to cause some slight adhesive wear in Fig. 7c, e. Some heavier damages of the inserts were found in Fig. 8 when a cutting speed of 350 m/min, a feed of 0.10 mm/r and a depth of cut of 0.30 mm were applied to turn the 321 austenitic stainless steel. In the region with the cutting edges, the edge chipping, which included a larger notch wear, was formed in Fig. 8a. It was a fracture texture without any adhesion inside the notch (see Fig. 8b), the fracture of the tool material inside the notch rooted deeply in the grains, and some dimples remained after some grains were pulled out. The damage was notably complex in the wear region with the flank face. First, a bulk of stainless steel was adhered on the flank face; second, some grooves were scored deeply on the flank face and third, some cross cracks were generated on the worn flank face (see Fig. 8c, d), which was distinguished from the formation of cracks on the worn flank face in machining the 17-4PH martensitic stainless steel; however, some

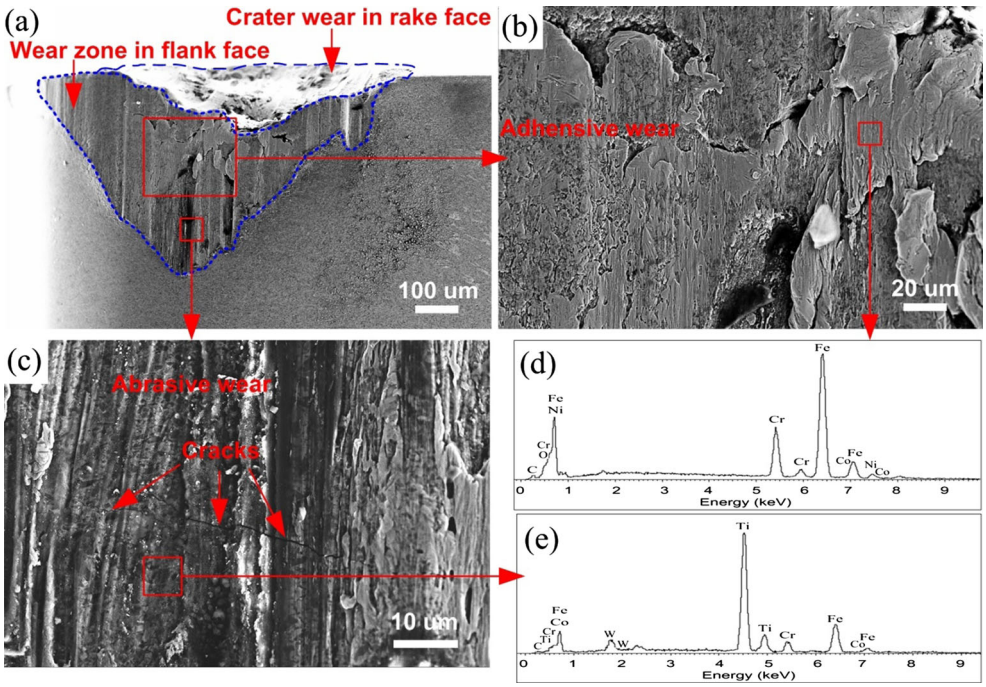

Fig. 5 SEM micrographs and EDS spectrums of the damage on the flank face of the inserts when machining 17-4PH martensitic stainless steel at v=400 m/min, f=0.10 mm/r and a_p=0.35 mm

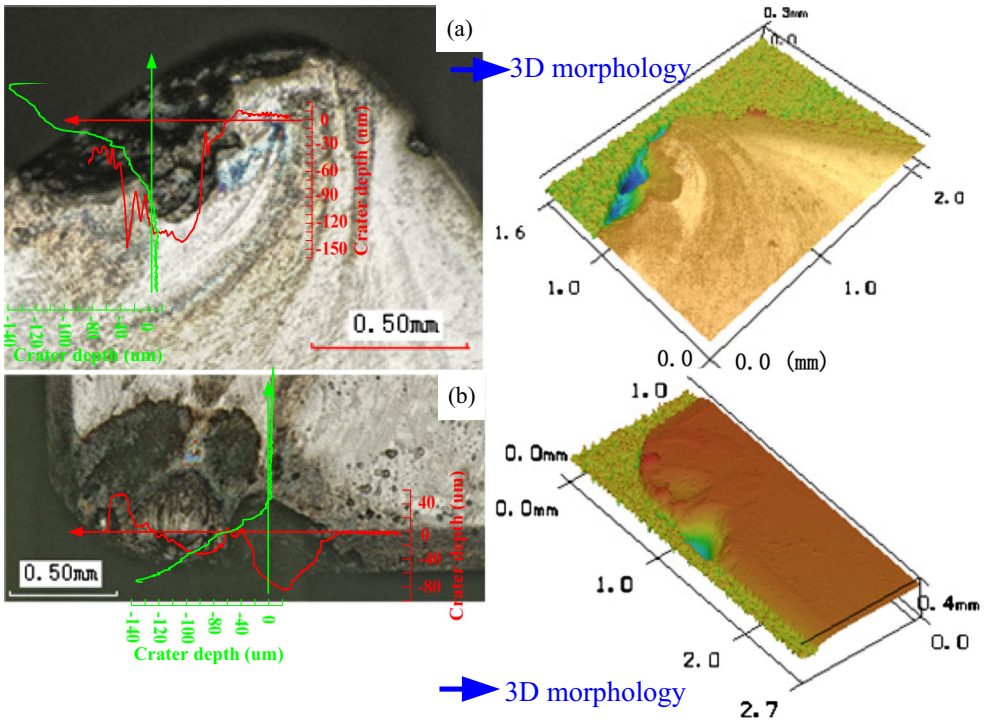

Fig. 6 LSM topographies of the damage on the rake face of the inserts when machining 321 austenitic stainless steel at **a** v=300 m/min, f=0.10 mm/r and a_p=0.35 mm and **b** v=350 m/min, f=0.10 mm/r and a_p=0.30 mm

cracks were terminated, and bridging occurred during its propagation because of the good mechanical properties of our developed tool material (see Fig. 8e). Because of these cracks, further cutting resulted in gross destruction of the inserts. A stronger oxygen peak was identified based on the EDS pattern in Fig. 8f, which indicates that the cutting created a great deal of heat so that the oxidation was accompanied with the tool wear.

Comparing the above results, it is found that the tool life was impaired when machining 321 austenitic stainless steel, although its cutting parameters were lower than those of 17-4PH martensitic stainless steel. Three differences between these two stainless steels can be summarised: (i) when the 17-4PH martensitic stainless steel was turned, the edge damage originated from the enlargement of a crater on the rake face, and its behaviour was outwear; on the contrary, the edge

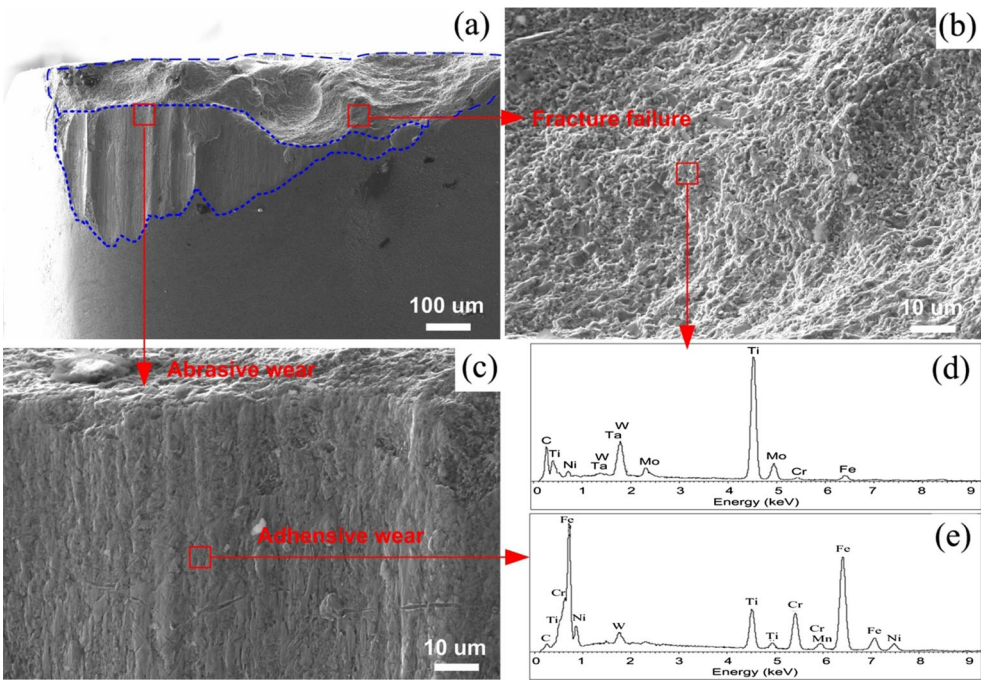

Fig. 7 SEM micrographs and EDS spectrums of the damage on the flank face of the inserts when machining 321 austenitic stainless steel at v=300 m/min, f=0.10 mm/r and a_p=0.35 mm

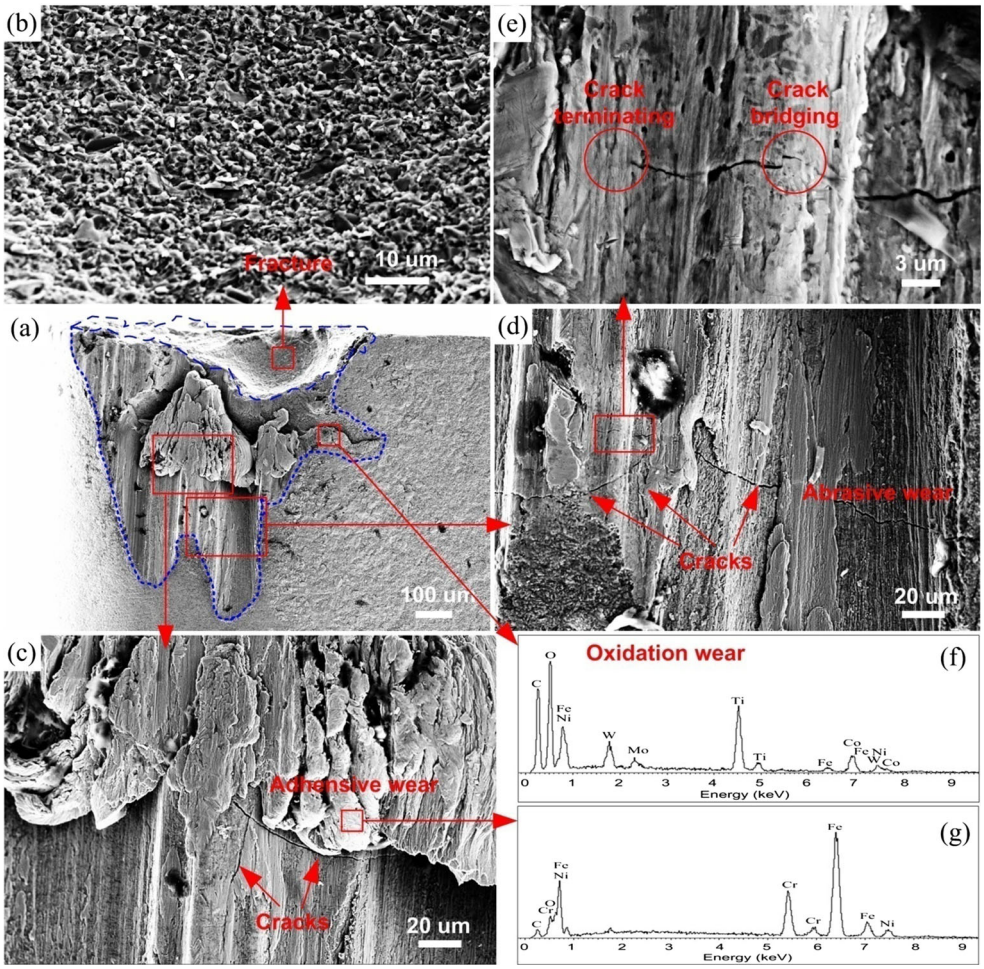

Fig. 8 SEM micrographs and EDS spectrums of the damage on the flank face of the inserts when machining 321 austenitic stainless steel at v=350 m/min, f=0.10 mm/r and a_p=0.30 mm

damage originated from a loss of edge strength, which was caused by the heavy notch wear when turning the 321 austenitic stainless steel, and it was a torn behaviour of chipping at the final failure; (ii) when machining the 17-4PH martensitic stainless steel, the flank face damage was predominated by the abrasive wear and slight adhesive wear for the lower cutting parameters, as demonstrated in our previous work [17], whereas for the higher cutting parameters, the abrasive wear was aggravated, and more workpiece material was attached on the flank face, as shown in this work. In the machining of the 321 austenitic stainless steel, the abrasive wear had some deep valleys and high ridges on the worn flank face, and the coincidence of heavy build-up adhesion was presented. Klim et al. [18] found that the adhesive phenomenon easily formed in the turning of the 17-4PH martensitic stainless steel. In this work, the adhesion more likely occurred in the turning of the 321 austenitic stainless steel; (iii) although cracks were generated on the worn flank face when machining these two stainless steels at high cutting speed, the steels exhibited different characteristics. The cracks were mutually parallel to the cutting speed direction and did not connect because of the resistance to crack propagation of hot-pressed sintering tool material when the 17-4PH martensitic stainless steel was machined, whereas the cracks interlaced when the 321 austenitic stainless steel was machined, that is, some cracks were parallel and others were perpendicular to the cutting speed direction. Although some mechanical properties of the 321 austenitic stainless steel, such as the yield strength, tensile strength and hardness, were inferior to those of the 17-4PH martensitic stainless steel, much worse tool damage in the machining of the 321 austenitic stainless steel were attributed to some of the changes in the mechanical properties of austenitic stainless steel, which resulted from the higher cutting heat. A tool temperature of approximately 800~900 °C was attainable in the orthogonal cutting of 316 austenitic stainless steel with a cutting speed of 180 m/min and a feed of 0.2 mm/r [19, 20]. The higher temperature should be expected when a higher cutting speed was applied to turn the 321 austenitic stainless steel in our work. The higher cutting heat developed a heavy work-hardening layer to deepen the attrition wear of the flank face and augmented the friction force between the flank face and the machined-surface. The formation of a heavy work-hardening layer was also responsible for the edge chipping when machining the 321 austenitic stainless steel. The higher

elongation of the 321 austenitic stainless steel aggravated the rubbing of the machined-surface with the cutting tool at the chip boundary to create the large notch, which acted as a facture origin to easily cause the edge chipping when the work-hardening layer was encountered. Many cracks on the work flank face were related to an extremely formidable cutting condition when machining the 321 austenitic stainless steel. The higher friction force produced a stretching force on the tool materials to initiate the cracks parallel to the cutting speed; however, the higher cutting heat generated a large gradient of thermal stress from the cutting zone to the non-cutting zone, which formed cracks perpendicular to the cutting speed. Thus, only the cracks parallel to the cutting speed appeared on the worn flank wear when the 17-4PH martensitic stainless steel was turned even with high cutting parameters (v= 400 m/min, f=0.10 mm/r, a_p=0.35 mm).

3.3 Machined-surface quality

Figure 9 shows the relationships between the machined-surface roughness and tool wear in the machining of two stainless steels at different cutting parameters. The roughness value increased with the volume rates of flank wear. The finished surface roughness was stable after the rapid tool wear and was enlarged at the time of total destruction. Under the same cutting conditions (v=400 m/min, f=0.10 mm/r, a_p= 0.35 mm), the tool wear and surface roughness exhibited some different behaviours. The values of surface roughness evolved more rapidly in machining of 321 austenitic stainless steel than 17-4PH martensitic stainless steel. Figure 9a, b also show that, to the same tool wear extent (about 0.8~0.9 or 0.14~0.16 mm), the machined-surface roughness of the 321 austenitic stainless steel is more than two times worse than that of the 17-4PH martensitic stainless steel. However, when the tool wear exceeded 0.2 mm, the machined-surfaces of these two stainless steels were coarsened quickly. Wang et al. [21] demonstrated that the presence of elastic recovery could produce a better finished surface by generating a lighter tool-nose cut scallop height in milling copper, aluminium alloy and aluminium bronze. The better plasticity of the 321 austenitic than 17-4PH martensitic stainless steels could engender a more plastic deformation which facilitated a coarse machined-surface. When the cutting speed was reduced from 400 to 300 m/min at the same feed and depth of cut for machining the 321 austenitic stainless steel, the tool life was approximately doubled. Comparing Fig. 9b and c, it is found that the machined-surface was smoother at the cutting speeds of 300 m/min than 400 m/min although their tool flank reached the same wearing capacities. For machining the austenitic stainless steel, the cutting force did not alter when the cutting speed increased from 300 to 400 m/min [22, 23], whereas the cutting heat caused by an increase of the cutting speed could be cumulated non-linearly near the cutting zone [20]. Though the cutting speed could take an advantage of the faster material removal rate and make the chip remove some cutting heat from the cutting zone, an amount of heat went back into the cutting tool itself. The higher cutting heat softened the cutting edge of inserts, and the sharpness of inserts

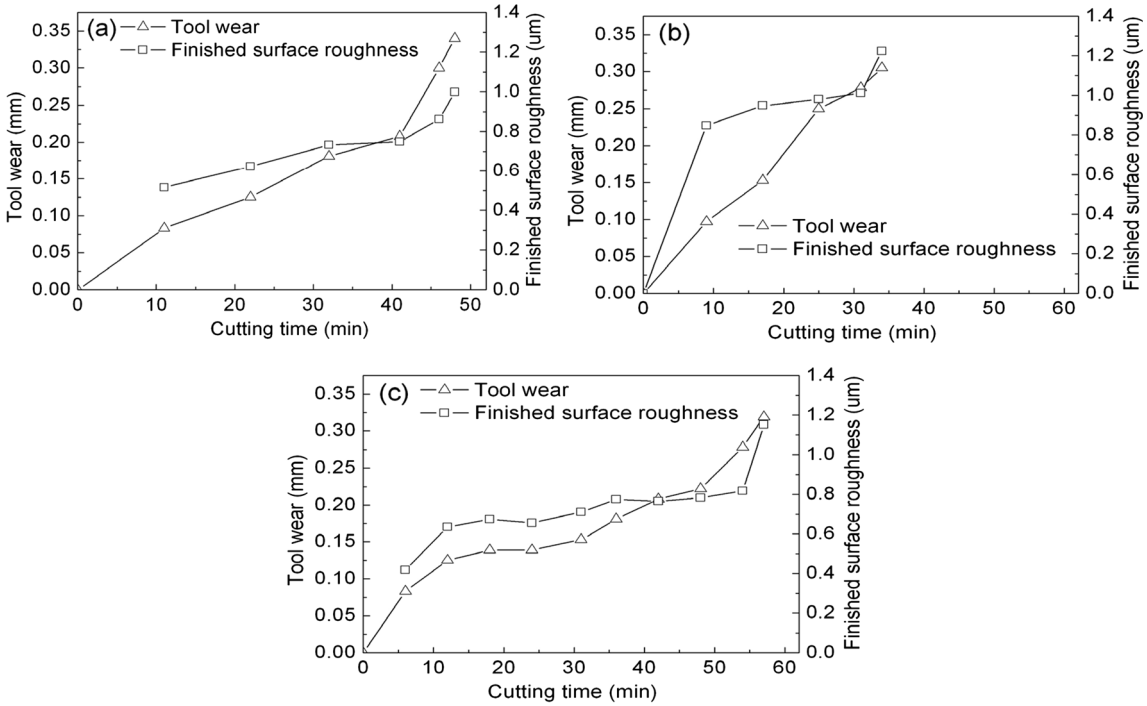

Fig. 9 Finished surface roughness vs. tool wear in the machining of **a** 17-4PH martensitic and **b** 321 austenitic stainless steels at v=400 m/min, f= 0.10 mm/r and a_p=0.35 mm and **c** 321 austenitic stainless steel at v=300 m/min, f=0.10 mm/r and a_p=0.35 mm

was depressed as a result. This can explain the reasons that the worse machined-surface roughness was obtained at higher cutting speed despite of the same tool wear capacity caused by the cutting speeds of 300 and 400 m/min. However, with our developed inserts, the finished surface has a smoothness of below 1.0 μm at the optimum cutting times for both stainless steels, which shows their good cutting performance.

A great deal of surface plucking, coating and matrix of tool and ferrous compounds were produced on the machined surface for some difficult-to-cut materials [24]. Because these two stainless steels used by our work were applied in corrosive environments, the topographies of their machined-surfaces are important to the performances of their parts if some defects existed on the machined surface. Figure 10 shows the SEM micrographs of the machined-surface topographies when two stainless steels were machined at different cutting parameters. No tool materials were obviously attached to the machined surface for either 17-4PH or 321 stainless steels. On the machined surface of 17-4PH martensitic stainless steel, some pits were observed; in particular, there was a certain amount of pits at the increased feed of 0.15 mm/r. Akasawa et al. [25] investigated the machinability of different austenitic stainless steels and found numerous pits in the deformed layer when the resulphurised 303 and 303Cu stainless steels were turned. They demonstrated that these pits were produced by sulphide inclusions in the stainless steel. In this work, the 17-4PH is a precipitation-hardening martensitic stainless steel with a high Cu content, where some slender inclusions are dispersed. When the cutting edge was plunged, cracks were initiated at the interface among the deformed bulk materials and inclusions or precipitates because of their different deformations. When the cutting proceeded, inclusions or precipitates detached from the severely deformed surface layer and pits were created on the machined-surface. In contrast with the 17-4PH martensitic stainless steel, some laps were observed on the machined-surface of the 321 austenitic stainless steel, which provides an evidence of a workpiece side flow because of its good plasticity. Similar effects were reported by other researchers in the dry turning of 303 austenitic stainless steel [8]. The material side flow could become more serious when the feed increased in the machining of the 321 austenitic stainless steel.

Further visualised topographies of machined-surfaces were presented for two stainless steels at different cutting parameters in Fig. 11. These surfaces were characterised by the peak-to-valley topography depending on the workpiece properties. Figure 11b shows that most of the previously discussed pits were produced on the ridges. These pits remained after the hard inclusion or precipitations were pulled out, which were wrapped under the chips and directly wore away the tool face. Because of the surface ridges in contact with the cutting edge at a distance from the tool tip, the tool face close to this edge was damaged so that the crater ultimately enlarged to the cutting edge. The edge destruction induced the total tool failure, which can explain the formation of tool damage on the rake face. Unlike the topographies of the machined-surface of the 17-4PH martensitic stainless steel, the machined-surface of the 321 austenitic stainless steel contained some local irregularities that resulted from the material side flow on the side of the ridges (see Fig. 11c, d). Kishawy et al. [26] demonstrated two mechanisms of material side flow: the material was squeezed between the tool flank and the machined-surface when the chip thickness was below a minimum value or the plasticised material in the cutting zone flew through the worn trailing edge to the side of the tool. Our work was consistent with their second mechanism because server damage was found on the trailing edge as discussed in section 3.2. An amount of attached 321 steel on the tool flank was closely

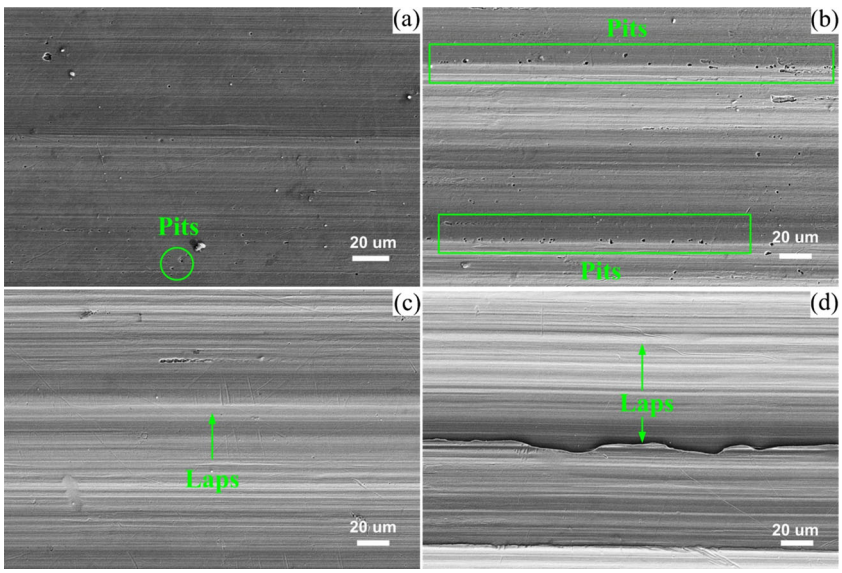

Fig. 10 SEM micrographs of the finished surface roughness when cutting 17-4PH martensitic stainless steel with **a** v=400 m/min, f=0.10 mm/r and a_p=0.35 mm (Ra=0.949 μm) or **b** v=350 m/min, f=0.15 mm/r and a_p=0.35 mm (Ra=1.736 um) and 321 austenitic stainless steel with **c** v=300 m/min, f=0.10 mm/r and a_p=0.35 mm (Ra=0.776 um) or **d** v=350 m/min, f=0.15 mm/r and a_p=0.35 mm (Ra=2.494 um)

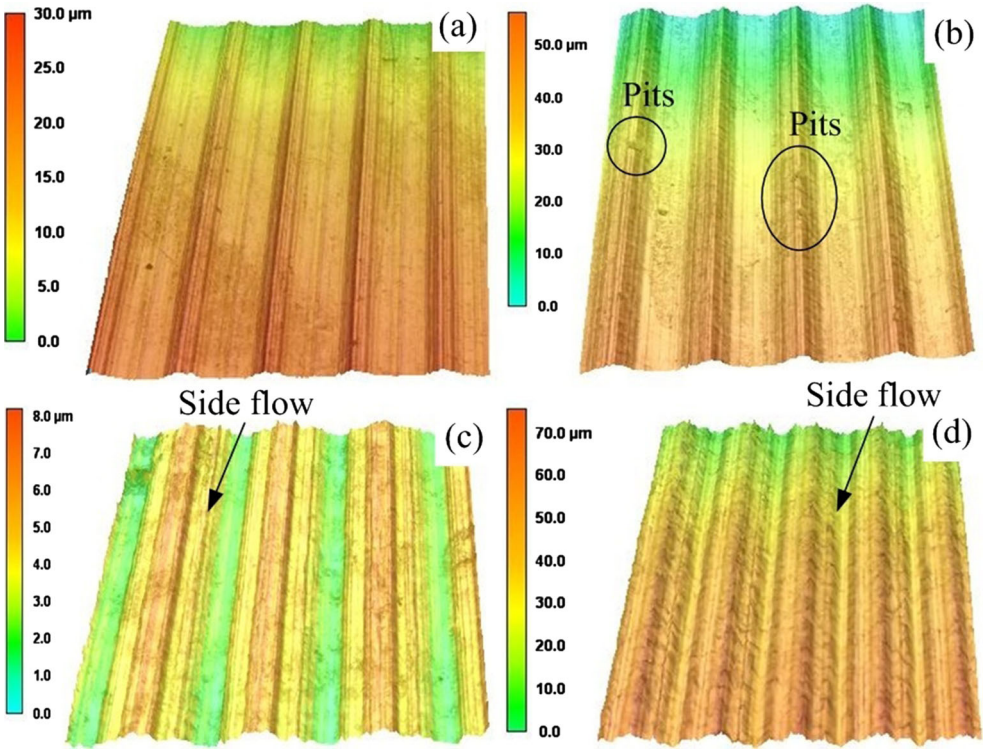

Fig. 11 LSM topographies of the finished surface roughness after cutting 17-4PH martensitic stainless steel with **a** v=400 m/min, f=0.10 mm/r and a_p=0.35 mm (Ra=0.949 μm) and **b** v=350 m/min, f=0.15 mm/r and a_p=0.35 mm (Ra=1.736 um) and 321 austenitic stainless steel with **c** v=300 m/min, f=0.10 mm/r, a_p=0.35 mm (Ra=0.776 um) and **d** v=350 m/min, f=0.15 mm/r, a_p=0.35 mm (Ra=2.494 um)

related to these side flows that occurred when the chip material in the cutting tool edge was exposed to high pressure and temperature, which produced a complete plasticisation. The plasticisation produced flows through the main cutting edge toward the secondary cutting edge and adhered on the new machined-surface; during this process, some 321 materials diffused onto the tool flank. The austenite near the machined-surface transformed to martensite when machining 304 austenitic stainless steel and a harder white layer than bulk material was formed [27], which increased with increasing the cutting speed and feed rate. The transformation from austenite to martensite was closely related to the higher temperature in cutting zone which ascribed to the plasticisation (side flow) of the machined surface. Therefore, the cutting insert encountered not only the adherence of side flow but also hardening of phase transformation of machined surface, and the tool life and surface qualities became worse quickly with increasing the cutting parameters for machining 321 austenitic stainless steel.

4 Conclusions

1. The cutting speed has the most dominant effect on the tool life during machining two stainless steels according to our deduced mathematical formulas. An increase of depth of cut availed the tool life to some extent because the cutting edge keeps away from the work-hardening layer in machining of 321 austenitic stainless steel. The used cutting parameters are as follows: a cutting speed of 350~400 m/min for 17-4PH steel and 300~350 m/min for 321 steel, a feed of 0.10 mm/r and a depth of cut of 0.30~0.35 mm, which is considered a notably efficient parameter to machine stainless steel. At this time, the tool life exceeded 46 min, and the finished surface roughness was below 1.0 μm. The longest tool life and the best surface roughness were 169 min and 0.58 μm, respectively, when machining the 17-4PH martensitic stainless steel at the cutting speed of 300 mm/min, feed of 0.1 mm/min, and depth of cut of 0.25 mm.

2. The edge damage was outworn because a crater on the rake face was enlarged in the machining of 17-4PH martensitic stainless steel, whereas the edge damage chipped as a result of a loss of edge strength, which was caused by the heavy notch and work-hardening layer in the machining of 321 austenitic stainless steel. The abrasion with deep valleys and high ridges and the serious adhesion more likely occurred when turning the 321 austenitic stainless steel. On the worn flank face, only parallel cracks were produced when machining the 17-4PH martensitic stainless steel, even with high cutting parameters, whereas many interlacing cracks were generated when machining the 321 austenitic stainless steel, which were attributed to some changes of the mechanical properties of austenitic stainless steel because of the high cutting heat and forces.

3. No tool material was attached on the machined-surface for both stainless steels. On the machined-surface of 17-4PH martensitic stainless steel, most pits were on the ridges because of some inclusions or precipitations dispersing in the workpiece

material. These pits caused the tool face near this edge to be damaged so that the crater ultimately enlarged to the cutting edge. On the machined-surface of the 321 austenitic stainless steel, there was evidence of material side flow on the side of the ridges because of its good plasticity. An amount of attached 321 steel on tool flank was closely related to these side flows, which occurred when the chip material in the cutting tool edge was exposed to high pressure and temperature.

Acknowledgments This project was supported by the Program for New Century Excellent Talents in University (NCET-13-0357), Tai Shan Scholar Foundation and the Natural Science Foundation of Shandong Province (ZR2014EEM026).

References

1. Peng Y, Miao HZ, Peng JX (2013) Development of TiCN-based cermets: mechanical properties and wear mechanism. Int J Refract Met Hard Mater 39:78–89
2. Qiu LK, Liu XK, Peng Y, Ma WM (2007) Types, performance and application of Al_2O_3 system ceramic cutting tool. J Rare Earth 25(2): 22–326
3. Shaw MC (2005) Metal cutting principle. Oxford University, New York
4. Liu XK, Qiu LK, Cui T (2007) Composition, characteristics and development of advanced ceramic cutting tools. J Rare Earth 25(2): 287–294
5. Kwon WT, June SP, Kang SH (2005) Effect of group IV elements on the cutting characteristics of Ti(C, N) cermet tools and reliability analysis. J Mater Process Technol 166(1):9–14
6. Wen TC, Chung ST (2003) The investigation on the prediction of tool wear and the determination of optimum cutting conditions in machining 17-4PH stainless steel. J Mater Process Technol 140(1–3):340–345
7. Xavior MA, Adithan M (2009) Determination the influence of cutting fluids on tool wear and surface roughness during turning of AISI 304 austenitic stainless steel. J Mater Process Technol 209(2):900–909
8. Fernadez AI, Barreiro J, Lopez LN, Martinez S (2011) Effect of very high cutting speed on shearing, cutting forces and roughness in dry turning of austenitic stainless steels. Int J Adv Manuf Technol 57(1–4):61–71
9. Noordin MY, Kurniawan D, Tang YC, Muniswaran K (2012) Feasibility of mild hard turning of stainless steel using coated carbide tool. Int J Adv Manuf Technol 60(9–12):853–863
10. Gerth J, Gustavsson F, Collin M, Andersson G, Nordh LG, Heinrich J, Wiklund U (2014) Adhesion phenomena in the secondary shear zone in turning of austenitic stainless steel and carbon steel. J Mater Process Technol 214(8):1467–1481
11. Grzesik W, Zak K (2012) Surface integrity generated by oblique machining of steel and iron parts. J Mater Process Technol 212(12): 2586–2596
12. Ren LQ (2003) Optimum design and analysis of experiments. Higher Education Press, Beijing
13. Lakhdar B, Smail B, Mohamed A, Salim B, Francois G (2014) Simultaneous optimization of surface roughness and material removal rate for turnining of X20Cr13 stainless steel. Int J Adv Manuf Technol 74(1–4):879–891
14. Farshid J, Hossein A, Mehdi F (2014) Improving surface intergrity in finish machining of Inconel 718 alloy using intelligent systems. Int J Adv Manuf Technol 71(5–8):817–827
15. Kumar AS, Durai AR, Sornakumar T (2006) The effects of tools wear on tool life of alumina-based ceramic cuttting tools while machining hardned martensitic stainless steel. J Mater Process Technol 173(2):151–156
16. Xiong J, Guo ZX, Yang M, Sj X, Chen JZ (2009) Effect of ultra-fine $Ti(C_{0.5}N_{0.5})$ on the microstructure and properties of gradient cemented carbide. Mater Process Technol 209(14):5293–5299
17. Zou B, Zhou HJ, Xu KT, Huang CZ, Wang J, Li SS (2014) Study of a hot-pressed sintering preparation of $Ti(C_7N_3)$-based composite cermets materials and their performance as cutting tools. J Alloys Compd 611:363–371
18. Klim Z, Ennajimi E, Balazinski M, Fortin C (1996) Cutting tool reliability analysis for variable feed milling of 17-4PH stainless steel. Wear 195(1–2):206–213
19. Noordin MY, Venkatesh VC, Sharif S (2007) Dry turning of tempered martensitic stainless tool steel using coated cermet and coated carbide tools. J Mater Process Technol 185(1–3):83–90
20. Rachid MS, Hariharan C (2012) Experimental study and modeling of tool temperature distribution in orthogonal cutting of AISI 316L and AISI 3115 steels. Int J Adv Manuf Technol 56(9–12):865–877
21. Wang SJ, To S, Cheung CF (2013) An investigation into material-induced surface roughness in ultra-precision milling. Int J Adv Manuf Technol 68(1–3):607–616
22. Maure PA, Fontraine M, Michel G, Thibaud S, Gelin JC (2013) Experimental investigations from conventional to high speed milling on a 304-L stainless steel. Int J Adv Manuf Technol 69(9–12):2191–2213
23. Palmai Z (2014) A model of non-linear cumulative damage to tools at changing cutting speeds. Int J Adv Manuf Technol 74(5–8):973–982
24. Zou B, Chen M, Li SS (2011) Study on finish-turning of NiCr20TiAl nickel-based alloy using Al2O3/TiN-coated carbide tools. Int J Adv Manuf Technol 53(1–3):81–92
25. Akasawa T, Sakurai H, Nakamura M, Tanaka T, Takano K (2003) Effects of free-cutting additives on the machinability of austenitic stainless steels. J Mater Process Technol 143–144:66–71
26. Kishawy HA, Elbestawi MA (1999) Effects of process parameters on material side flow during hard turning. Int J Mach Tools Manuf 39(7):1017–1030
27. Yan L, Yang WY, Jin HP, Wang ZG (2012) Analytical modeling of microstructure changes in the machining of 304 stainless steel. Int J Mach Tools Manuf 58(1–4):45–55